SCIENCE CHINA Materials

ARTICLES

mater.scichina.com link.springer.com

Published online 18 August 2016 | doi: 10.1007/s40843-016-5066-y
Sci China Mater 2016, 59(10): 833–841

SPECIAL ISSUE: Excitonic Solar Cells (II)

Ultrathin ALD coating on TiO_2 photoanodes with enhanced quantum dot loading and charge collection in quantum dots sensitized solar cells

Ting Shen[1], Jianjun Tian[1*], Bo Li[1] and Guozhong Cao[1,2*]

ABSTRACT TiO_2 nanocrystals are widely used in photoanodes for quantum dot solar cells (QDSCs) owing to their chemical stability and suitable energy band structure. However, surface defects and grain boundaries of TiO_2 nanocrystals photoanodes allow high surface charge recombination, which limits the performance of QDSCs. In this work, an ultrathin TiO_2 layer is introduced to the surface of TiO_2 photoanodes by atomic layer deposition (ALD). The ultrathin layer not only reduces the surface defects of TiO_2 nanoparticles and strengthens the connection between adjacent nanoparticles to suppress the charge recombination for improving the electron collection efficiency (η_{cc}), but also increases the surface energy of photoanodes to load more quantum dots (QDs) for enhancing the light harvesting efficiency (LHE). As a result, the solar cell based on CdS/CdSe QDs with ALD treatment exhibits an efficiency of 5.07% that is much higher than that of the cells without modification (4.03%).

Keywords: CdS/CdSe, atomic layer deposition, quantum dots solar cells, charge recombination, electron collection

INTRODUCTION

As one of the third generation solar cell, quantum dot solar cells (QDSCs) [1] based on wide bandgap oxide semiconductors and inorganic quantum dots have attracted extensive research efforts in industry and academia [2,3]. QDSCs generally consist of five main components [4]: fluorine doped tin oxide (FTO) glass or indium doped tin oxide (ITO) glass as the substrate to collect and transport charges, mesoporous photoanode film made of wide band-gap oxide semiconductor nanoparticles as scaffold to load quantum dots (QDs) sensitizers, a self-assembled monolayer of QDs as sensitizers, polysulfide electrolyte (S^{2-}/S_n^{2-}) as the hole transporting media, and counter electrode to collect charges and catalyze the redox reaction in electrolyte. Analogue to dye-sensitized solar cells, wide bandgap semiconductor oxides, such as TiO_2 [5,6], ZnO [7], SnO_2 [8], have been used to make mesoporous photoanodes in QDSCs. Among these materials, TiO_2 has been extensively applied to the photoanodes of QDSCs, owing to its excellent chemical stability [9], high charge mobility [10] and suitable band-structure [11]. However, TiO_2 nanostructure still contains lots of surface defects that lead to a side reaction–charge recombination [12], which reduces the power conversion efficiency (PCE) of QDSCs based on TiO_2 photoanodes.

Thus, surface modification of TiO_2 photoanode is considered as one of effective and reliable approaches to overcome this issue. $TiCl_4$ was usually introduced in TiO_2 films to form a blocking layer, which suppressed the dark current and led to an increase in open circuit voltage for the cells [13]. Palomares *et al.* [14] reported a methodology for conformally coating nanocrystalline TiO_2 films with a thin overlayer of a second metal oxide (Al_2O_3, ZrO_2 or SiO_2) by dipping each TiO_2 film in a solution of suitable precursors. They found that Al_2O_3 was optimal for retarding interfacial recombination losses and the overall device efficiency had a 35% improvement. Recently, we developed a ZnO/TiO_2 structure for QDSCs by a facile chemical passivation strategy [7,15]. This strategy that combines the selective etching of ZnO from the convex surface and uniform deposition of TiO_2 nanoparticles not only enlarged the aperture in ZnO photoanode but also depressed the surface defects because

[1] Institute of Advanced Materials and Technology, University of Science and Technology Beijing, Beijing 100083, China
[2] Department of Materials and Engineering, University of Washington, Seattle 98195-2120, USA
[*] Corresponding authors (emails: tianjianjun@mater.ustb.edu.cn (Tian J); gzcao@u.washington.edu (Cao G))

of the thin TiO_2 film as well as increased QDs loading. Finally, the QDSC based on ZnO with such modification exhibited a high PCE of 4.68%. In addition to the approaches described above, atomic layer deposition (ALD) has been regarded as one of ideal interface modification processes for the nanostructure and nanomaterial.

ALD is a vapor-phase deposition technique to grow homogeneous ultrathin films or conformal coating in a reaction chamber [16] due to its unique self-limiting nature [17], low growth temperature [18], precise control on film thickness [19] and large deposition area [20], making it as a popular and useful technology for fabricating complex nanostructures and investigating the properties of nanomaterials [21]. ALD has also been extensively applied and studied for surface modification in solar cell, which can be summarized into the following four aspects [22]: (a) fabrication of mesoporous photoanodes [19,20] for high loading of sensitizer and better charge transfer; (b) surface modification [23,24] to passivate trapping states; (c) introduction of catalytic noble metals [25] and (d) formation of desired heterojunction [26].

This paper reports the introduction of an ALD layer to modify the surface of TiO_2 photoanode for reducing the trapping state, increasing the surface energy to load more QDs and improving the charge collection efficiency in QDSC. An ultrathin TiO_2 layer was deposited on the surface of the mesoporous TiO_2 films for different cycles and the deposition rate was about 0.05 nm per cycle. The surface properties of the resulting photoanodes and the photoelectric conversion performance of the solar cells were investigated. The PCE of the device with ALD-treatment reaches 5.07% that is much higher than that of the device without ALD treatment (4.03%).

EXPERIMENTAL SECTION

Materials

Cadmium nitrate tetrahydrate ($Cd(NO_3)_2{\cdot}4H_2O$, Alfa Aesar, 98.5%), sodium sulphide nonahydrate ($Na_2S{\cdot}9H_2O$, Aladdin, ≥98.0%), sodium sulfite anhydrous (Na_2SO_3, Guoyao China, ≥97.0%), selenium powder (Se, Alfa Aesar, 99.0%), cadmium acetate dehydrate ($Cd(CH_3COO)_2$, Alfa Aesar, 98.0%), nitrilotriacetic acid trisodium salt monohydrate ($N(CH_3COONa)_3$, Alfa Aesar, 98.0%), sublimed sulfur (S, Guoyao China, ≥99.5%), zinc nitrate hexahydrate ($Zn(NO_3)_2{\cdot}6H_2O$, Aladdin, 99.0%), hydrochloric acid (HCl, Beijing China, 36%–38%), methanol anhydrous (CH_3OH, Guoyao China, ≥99.5%), TiO_2 (Degussa P25), and copper foil were used directly without further purification.

Photoanode preparation

The mesoporous photoanodes were fabricated according to our previous work [27]. The P25 powder was mixed with ethyl cellulose and α-terpilenol to form paste (in a rate of 1.8:0.9:7.3). Then the TiO_2 films were fabricated on the FTO (8 Ω/square) glass substrates with the doctor blade method. After 20 min at room temperature, the prepared films were sintered at 500°C (2°C min^{-1}) for 30 min to remove any organic matter and promote the crystallization. Finally, nearly 12 μm-thick TiO_2 film was obtained. Then the PICOSUN / SUNALE R-200 ALD System was utilized to deposit ultrathin TiO_2 layer on the surface of mesoporous TiO_2 films at 300°C. Titanium tetrachloride ($TiCl_4$) and H_2O were used as precursors with high purity nitrogen as a carrier and purging gas. Amorphous films grew at temperature below 165°C; anatase structure was observed at 165°C–350°C; and when the temperature was more than 350°C, rutile dominated in the films obtained [19]. The thickness of TiO_2 layers were 0.5 nm, 1.0 nm and 1.5 nm for coating of 10 cycles, 20 cycles and 30 cycles, respectively. Finally, the films were annealed at 500°C in air for 30 min.

Device fabrication

The interface-modified TiO_2 photoanodes were assembled with CdS QD by our previously reported method [27]. In brief, the TiO_2 films were first immersed into Cd^{2+} precursor solution for 1 min and immersed in S^- precursor solution, then rinsed with methanol and dried with air between each step. After 5 cycles of SILAR process, the photoanodes were immersed into an aqueous solution containing 0.1 mol L^{-1} Se, Na_2SO_3, $Cd(CH_3COO)_2$ and $N(CH_3COONa)_3$ for 3 h (under dark condition) at room temperature to deposit sufficient CdSe QDs. The electrolyte in this study was a liquid admixture of S^{2-}/S_n^{2-}, which was prepared from 1.0 mol L^{-1} S and 1.0 mol L^{-1} Na_2S solution dissolved in 7:3 methanol-water solution. The compact Cu_2S layer on the brass foil was used as the counter electrode. The active area of the QDSC was 0.196 cm^2.

Photovoltaic characterization

A Shimadzu UV-3600 UV–vis–NIR spectrophotometer was used to measure QD absorption spectrum. The surface energy spectra were analyzed using inverse gas chromatography surface energy analyzer (IGC SEA). The incident photon to current conversion efficiency (IPCE) spectra were obtained in the range of 400–700 nm using a Keithley 2400 multimeter with illumination of a 300 W tungsten lamp with a Spectral Product DK240 monochromator.

The characteristic *J-V* curves were measured with the same instrument used for IPCE measurements under AM 1.5 G illumination provided by a solar simulator (Crowntech, SOL02 series). The N_2 adsorption-desorption isotherm curve were carried out with a surface and porosity analyzer (Micromerities, ASAP 2020). The electrochemical workstation was also used to measure the electrochemical impedance spectroscopy (EIS). Intensity modulated photocurrent/photovoltage spectra (IMPS/IMVS) measurements were carried out with the electrochemical workstation (Germany, Zahner Company), using light emitting diodes driven by Expot (Germany, Zahner Company).

RESULTS AND DISCUSSION

Fig. 1a compares the *J-V* characteristics of the QDSCs with respect to the number of TiO_2 ALD cycles and the corresponding parameters of the solar cells are summarized in Table 1, including open circuit voltage (V_{oc}), short circuit current density (J_{sc}), fill factor (FF) and power conversion efficiency (PCE). Under the illumination, the properties of the QDSCs with 20 cycles-ALD are 0.597 V of V_{oc}, 13.19 mA cm^{-2} of J_{sc}, 64.41% of FF and 5.07% of PCE, which display the best performance in comparison with 11.69 mA cm^{-2} and 4.03% for the QDSCs without ALD treatment, 12.19 mA cm^{-2} and 4.41% for the QDSCs with 10 cycles-ALD, and 11.65 mA cm^{-2} and 4.53% for the QDSCs with 30 cycles-ALD. V_{oc} and FF for the devices with ALD treatment also show the same trend like J_{sc} and PCE. So the performance of the QDSCs increases firstly and then decreases as cycles of the ALD increase. It demonstrates that the introduction of the ultrathin layer of TiO_2 on the surface of TiO_2 mesoporous film by ALD can improve the performance of QDSCs. When the cycles are more than 20, the ultrathin layer is too thick, which reduces the porosity and specific surface area of the photoanode, leading to the decrease of QDs loading and consequently J_{sc}. Approximating the TiO_2-coated structure as a series of the interconnected spheres and cylinders, the surface area should increase linearly with TiO_2 deposited. However, the surface area decreases firstly and then increases, because of filling in the defect on the TiO_2 film [28]. To understand the effects of ALD ultrathin layer on light harvesting, electron transport and collection in the QDSCs, further characterization and discussion have been focused on the devices either without ALD treatment (denoted as w/o-ALD cell) or with 20 cycles ALD-treatment (w-ALD cell).

Fig. 1b compares incident photon to the charge carrier efficiency (IPCE) spectra of both solar cells. It is clear that the IPCE value of the w-ALD cell is higher than that of the w/o-ALD cell over the full range of entire wavelengths, suggesting a higher photocurrent in the device with ALD treatment. These characteristic corroborates well with the *J-V* curves (Fig. 1a). IPCE stands for the ratio of the electron number and the incident monochromatic photon number per unit time, which is determined by light harvesting efficiency (LHE), electron injection (Φ_{inj}) and charge collection efficiency (η_{cc}). Thus, the IPCE can be expressed by the following equation [29]:

$$\mathrm{IPCE} = \mathrm{LHE} \times \Phi_{inj} \times \eta_{cc}. \quad (1)$$

Fig. 2a shows the UV-vis absorption spectra of the TiO_2 photoanodes with and without ALD coating, and with and without CdS/CdSe QDs. For the TiO_2 films with and without ALD coating loaded with QDs (the solid lines), the absorption onsets approximate to each other in both curves and the absorption of the w-ALD sample is higher than that of the w/o-ALD sample. The two absorbance curves of bare

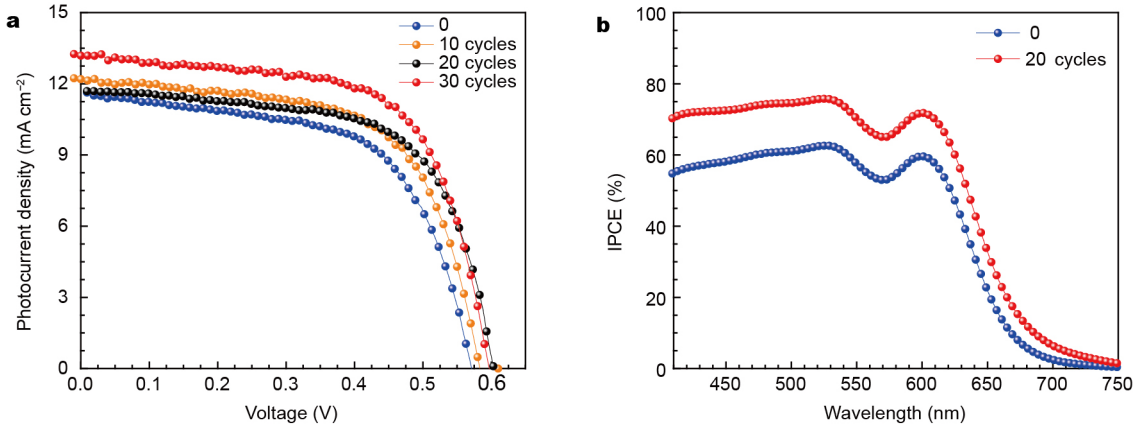

Figure 1 (a) *J-V* characteristics under illumination (one sun light intensity with AM 1.5G filter, measured under reverse scan condition) and (b) IPCE values for the CdS/CdSe QDSCs with and without ALD treatment.

Table 1 Summarized *J-V* characteristics of the CdS/CdSe QDSCs with and without ALD treatment[a)]

Samples	J_{sc} (mA cm^{-2})	V_{oc} (V)	FF (%)	η (%)
0	11.69	0.570	60.49	4.03±0.14
10 cycles	12.19	0.583	62.01	4.41±0.16
20 cycles	13.19	0.597	64.41	5.07±0.19
30 cycles	11.65	0.602	64.73	4.53±0.08

a) The standard deviation of the properties is based on the data of five cells in parallel.

TiO_2 films with and without ALD treatment overlaps each other (the dash lines). It demonstrates ALD has little effect on the light absorption of bare TiO_2 films. The high absorbance of w-ALD sample (the red solid line) indicates that the photoanode with ALD treatment can load more QDs and renders a competitive capability of photon absorption. To support this assumption, LHE, surface area and surface energy of the samples were further studied. LHE characteristics of the QDSCs were collected as shown in Fig. 2b. The LHE of the w-ALD sample was also observed to be higher than that of the w/o-ALD sample, which benefits to the photocurrent short density of the w-ALD devices [30]. For QDSCs, the surface properties of TiO_2 photoanodes play a key role in the amount of QDs loaded that decides the photocurrent. Nitrogen adsorption-desorption isotherms were measured and the results are shown in Fig. 2c, the inset exhibits the BJH (Barrett-Joyner-Halenda) pore size distribution of TiO_2 films with and without ALD treatment, and the corresponding parameters are summarized in Table 2. The pore volume decreases with the ALD treatment from 134.41 to 125.5 m^3 g^{-1}, as ALD TiO_2 fills some pore space in photoanode. In QDSCs, the average pore size and size distribution are known to affect the loading and distribution of QDs [7,31]. In general, the adsorbed amount of QDs would be reduced with the decrease of the mesopore size, but the results in this experiment are different. Firstly, the surface area of the film with ALD treatment is 47.81 m^2 g^{-1}, which is slightly higher than

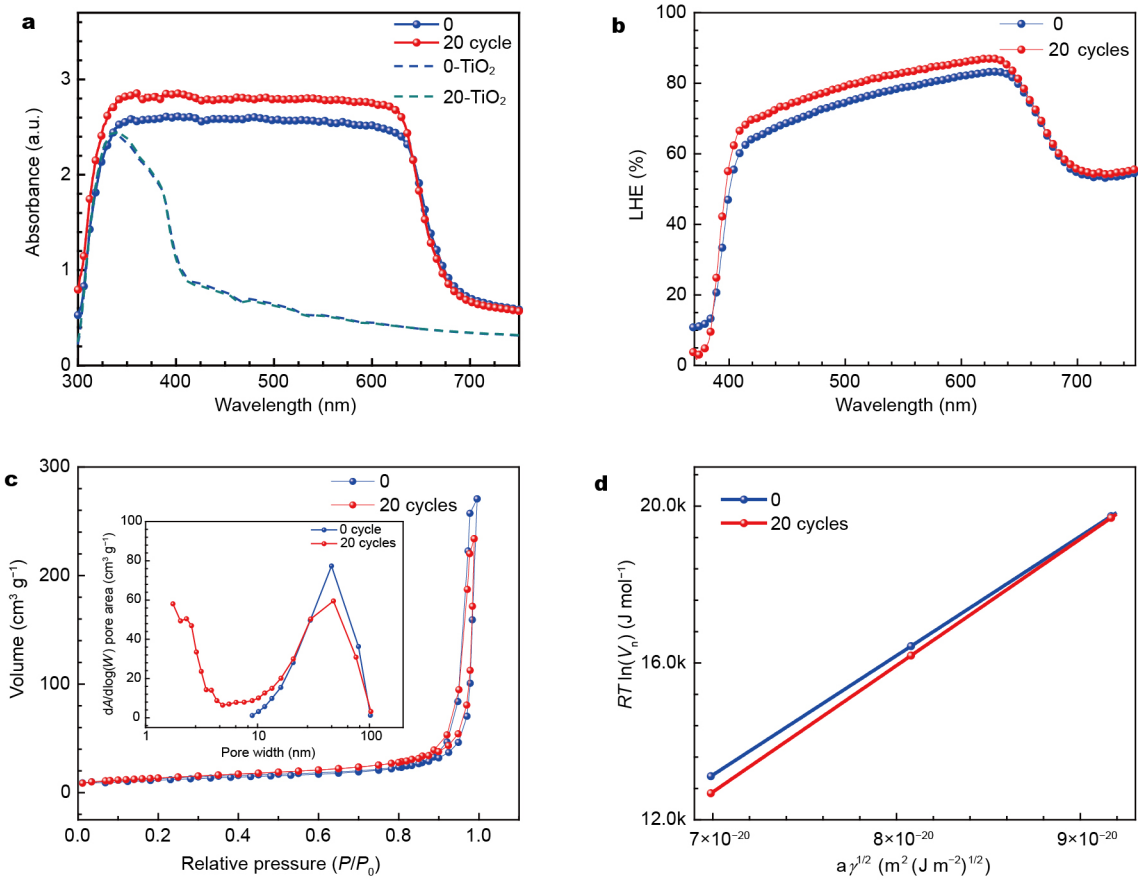

Figure 2 (a) Absorption spectra of TiO_2 photoanodes with and without ALD coating (the dash lines), and the TiO_2 films with and without ALD coating loaded with QDs (the solid lines). (b) Light harvesting efficiency of TiO_2 film with and without ALD coating loaded with CdS/CdSe QDs. (c) Nitrogen sorption isotherms (inset: BJH pore size distribution plots) and (d) Surface energy spectra of the TiO_2 particle with and without ALD treatment.

Table 2 The multi-point Brunauer–Emmett–Teller (BET) characteristics and the surface energy analysis properties of the TiO_2 particle with and without ALD treatment

Samples	BET surface area ($m^2\ g^{-1}$)	Pore volume ($m^3\ g^{-1}$)	Surface energy ($mJ\ m^{-2}$)
0	44.64	134.41	68.25
20 cycles	47.81	125.50	73.59

that of the sample without ALD treatment (44.64 $m^2\ g^{-1}$), implicating the change of the surface area is insignificant in this study. In addition, the surface energy of the mesoporous TiO_2 with ALD coating may change, which is another key factor for the loading of QDs. In order to find out the reason, the inverse gas chromatography surface energy analyser (IGC SEA) measurement was adopted to analyze the surface energy of the TiO_2 films with and without ALD treatment as SEA is specifically designed to measure surface energy heterogeneity [32,33]. The surface energy can be calculated by the following equation [31]:

$$RT\ln(V_n) = (r_s^d)^{1/2} \cdot 2Na(r_l^d)^{1/2} + K, \quad (2)$$

where r_s^d is the dispersive component of the surface energy. The r_l^d can be obtained from the linear slope of $RT\ln(V_n)$ *vs.* $(r_s^d)^{1/2}\ 2Na$. The SEA value for the TiO_2 with ALD treatment is 73.59 mJ m^{-2} that is higher than the value of 68.25 mJ m^{-2} for the TiO_2 without ALD treatment (Fig. 2d). The high value implies high surface activity. More QDs tend to deposit on the surface with high energy to decrease the energy of the whole system. The higher surface energy may be attributed to the fact that the surface of ALD TiO_2 coating became rough when converted from amorphous to crystalline, while the TiO_2 nanocrystals commonly possess near thermodynamic equilibrium shape. Therefore, ALD treatment can increase the loading of QDs, although the porosity of photoanodes decreases slightly. This result is also consistent with the LHE spectra (Fig. 2b). It can be seen that the increase of LHE is notable. In addition to LHE, the improvement of PCE of the QDSCs by ALD treatment may be attributed to the enhancement of η_{cc} or Φ_{inj}.

Absorbed photon to current conversion efficiency (APCE) can evaluate the η_{cc} and Φ_{inj} of the solar cells clearly, as the LHE has been ruled out [34]. The APCE of the w-ALD solar cell is found to be higher than that of the w/o-ALD solar cell throughout the entire range of wavelengths studied (Fig. 3), demonstrating that the ALD treatment is helpful for improving the conversion efficiency of the absorbed photons to electron-hole pairs. It is known that the driving force for the electron injection from QDs to the conduction band of TiO_2 is determined by the Fermi level of TiO_2/QDs [35]. An ultrathin coating on TiO_2 mesoporous films by ALD is impossible to change the band gap structure, evident from the absorption spectral (Fig. 2) as the absorption edges have not shown any detectable shift. So Φ_{inj} of the samples with and without ALD treatment would have no significant difference. It is clear that the enhancement of PCE for the QDSCs by ALD treatment is resulted from the high LHE and η_{cc}.

To further understand the electron transport and collection in the QDSCs with and without ALD treatment, EIS is carried out under dark condition with a forward bias of −0.55 V as shown in Fig. 4. The impedance related to the charge transfer process at the TiO_2/QDs/electrolyte interfaces can be described by the intermediate frequency semicircle (R_{ct}) and constant phase elements (CPE2) [36]. The results show that the values of R_{ct} corresponding to the devices with and without ALD treatment are 35 and 16 Ω, respectively. The increase of R_{ct} implies less electron-hole recombination at the interface of the TiO_2/QDs/electrolyte [37], which can lead to high V_{oc} and FF. The possible reason is that the ultrathin TiO_2 layer modifies the surface of TiO_2 nanoparticles to reduce trapping state defects in TiO_2 nanoparticles [38]. Furthermore, the improved interconnection in TiO_2 photoelectrode benefits to electrons transfer and inhibits the recombination [39]. Fig. 4b shows the corresponding Bode phase plots for the cells with and without ALD treatment. The electron lifetime (τ_r) can be obtained from the curve peak of the spectrum according to

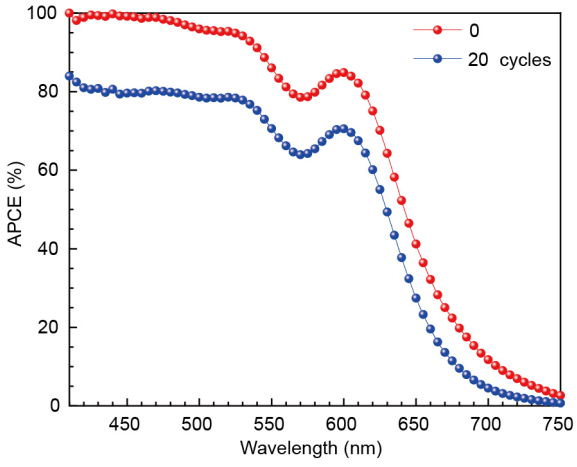

Figure 3 APCE curves of the CdS/CdSe QDSCs with and without ALD treatment.

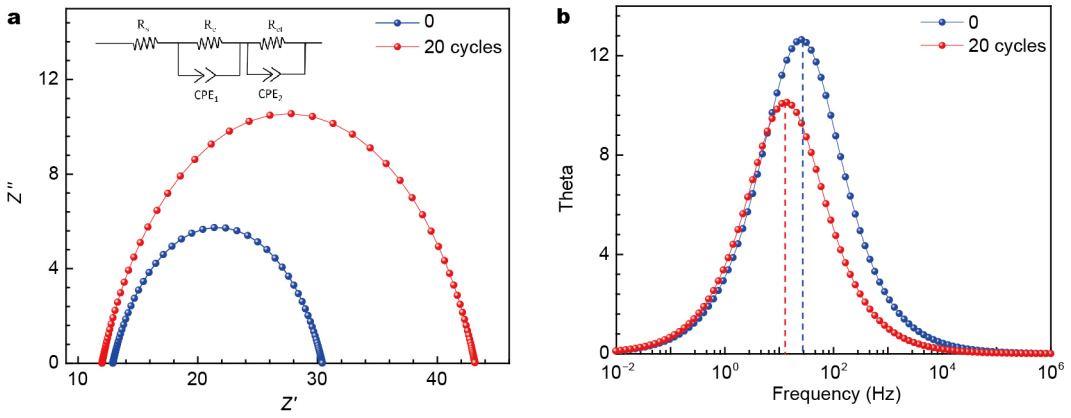

Figure 4 (a) Nyquist plot curves and (b) Bode plot curves of the QDSCs with respect to the number of TiO_2 ALD cycles under forward bias (−0.55 V) and dark condition.

the equation [40]:

$$\tau_r = 1/(2\pi f_{min}), \quad (3)$$

where f_{min} is the peak frequency in the Bode plot. The τ_r value of the w-ALD cell is 13.3 ms that is almost twice of 6.4 ms in the w/o-ALD cell. It is clear that the electron lifetime is prolonged by depositing the TiO_2 layer on the surface of the TiO_2 films, indicating a much slower recombination rate in the w-ALD cell. According to the results and discussion above, the effect of the ultrathin TiO_2 layer in the QDSC can be illustrated in Scheme 1. Upon illumination of the light, QDs can absorb photons to excite electron-hole pairs. The optimal electron injection can only proceed from the conduction band of QD to the conduction band of TiO_2 and then transfer to external circuit. However, there are always several recombination ways that are not beneficial (the red dash lines in Scheme 1). Because of the existence of the ultrathin TiO_2 layer deposited by ALD method, the surface trapping states were reduced to decrease the charge recombination of QD/TiO_2 and TiO_2/electrolyte as shown in Scheme 1. Thus, the effective number of the electron transfer to the external circuit can be increased.

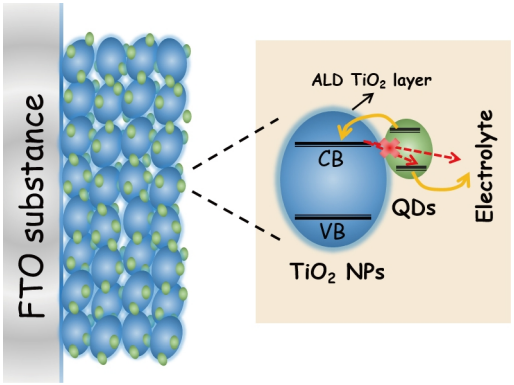

Scheme 1 Photoelectric conversion and recombination process in solar cells with ALD treatment.

The effect of surface modification on charge carrier dynamics of QDSCs with and without ALD treatment are investigated by intensity modulated photocurrent spectroscopy (IMPS) and intensity modulated photovoltage spectroscopy (IMVS). The time constant of electron transport (τ_d) and electron lifetime (τ_r) can be calculated by IMPS and IMVS frequency data according to the following equations [39]:

$$\tau_d = 1/(2\pi f_d), \quad (4)$$

$$\tau_r = 1/(2\pi f_r), \quad (5)$$

where f_d and f_r are the frequency of the minimum of the semicircle in the IMPS and IMVS plots, respectively. Fig. 5a shows that the τ_r of the w-ALD cell is higher than that of the w/o-ALD cell, suggesting that the former has a longer electron lifetime compared with that of the latter, while the electron transport times (τ_d) would be almost similar for the two devices. This can be attributed to the low recombination in the w-ALD cell. It is also thought that higher τ_r for the w-ALD cell could account for relatively higher V_{oc} and FF than those of the w/o-ALD cell. In order to elucidate the origin of the enhanced J_{sc}, the electron diffusion coefficient (D_n) and electron diffusion length (L_n) are calculated as following equations [39,41]:

$$D_n = d^2/2.35\tau_d, \quad (6)$$

$$L_n = (D_n\tau_r)^{1/2}, \quad (7)$$

where d is the thickness of the film. The w-ALD cell shows much longer diffusion length in comparison with the w/o-ALD cell, which indicates ALD treatments improve the connection between the adjacent TiO_2 particles, which

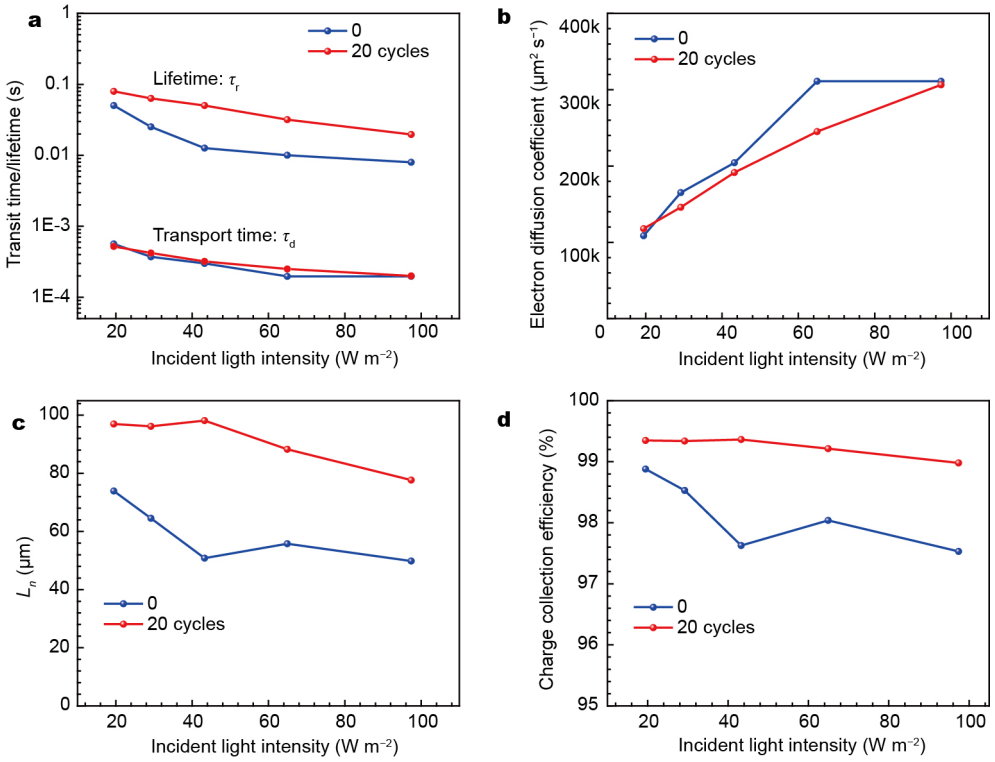

Figure 5 (a) Electron transport time and electron lifetime, (b) electron diffusion coefficient, (c) electron diffusion length and (d) effective charge collection efficiency of the CdS/CdSe QDSCs with and without ALD treatment as a function of the incident light intensity.

benefits the charge transport to reduce the charge recombination and increase the photocurrent. The plot of η_{cc} as a function of photocurrent is shown in Fig. 5d. The η_{cc} of the w-ALD cell is obtained over the light intensities from 19.48 to 97.38 W m^{-2}. The improvement in the η_{cc} (increased from 97% for w/o-ALD cells to 99% for w-ALD cells at 97.38 W m^{-2} of light intensity) shows that the presence of the ultrathin TiO_2 layer improves inter-particle connectivity and prevents the loss of photo-generated electron from the photoanode films to electrolyte.

CONCLUSIONS

An ultrathin ALD layer on the surface of TiO_2 photoanodes has demonstrated high power conversion efficiency of the resultant QDSCs. Both the surface area and energy were increased that resulted in more amounts of QDs loaded on the photoanodes. The impact of surface defects was notably suppressed and the connectivity between adjacent TiO_2 nanocrystals was enhanced, which benefits the charge transport with reduced charge recombination. As a result, the PCE of the QDSCs with ALD was up to 5.07%, which is much higher than that of the devices without ALD treatment (4.03%). The improvement of PCE for the QDSCs with ALD was mainly derived from the enhancement of LHE and η_{cc}.

Received 9 May 2016; accepted 1 June 2016; published online 18 August 2016

1 Kamat PV. Quantum dot solar cells. The next big thing in photovoltaics. J Phys Chem Lett, 2013, 4: 908–918
2 Tian J, Cao G. Control of nanostructures and interfaces of metal oxide semiconductors for quantum-dots-sensitized solar cells. J Phys Chem Lett, 2015, 6: 1859–1869
3 Tian J, Cao G. Design, fabrication and modification of metal oxide semiconductor for improving conversion efficiency of excitonic solar cells. Coordination Chem Rev, 2016, 320-321: 193–215
4 Carey GH, Abdelhady AL, Ning Z, *et al.* Colloidal quantum dot solar cells. Chem Rev, 2015, 115: 12732–12763
5 Du Z, Zhang H, Bao H, *et al.* Optimization of TiO_2 photoanode films for highly efficient quantum dot-sensitized solar cells. J Mater Chem A, 2014, 2: 13033–13040
6 Zhang J, Li S, Yang P, *et al.* Deposition of transparent TiO_2 nanotubes-films via electrophoretic technique for photovoltaic applications. Sci China Mater, 2015, 58: 785–790
7 Tian J, Zhang Q, Uchaker E, *et al.* Architectured ZnO photoelectrode for high efficiency quantum dot sensitized solar cells. Energy Environ Sci, 2013, 6: 3542–3547
8 Wang Y, Tian J, Fei C, *et al.* Microwave-assisted synthesis of SnO_2 nanosheets photoanodes for dye-sensitized solar cells. J Phys Chem C, 2014, 118: 25931–25938
9 Kamat PV. TiO_2 nanostructures: recent physical chemistry advances. J Phys Chem C, 2012, 116: 11849–11851
10 Chong B, Zhu W, Liu Y, *et al.* Highly efficient photoanodes based

on cascade structural semiconductors of $Cu_2Se/CdSe/TiO_2$: a multifaceted approach to achieving microstructural and compositional control. J Mater Chem A, 2016, 4: 1336–1344
11 Toyoda T, Shen Q. Quantum-dot-sensitized solar cells: effect of nanostructured TiO_2 morphologies on photovoltaic properties. J Phys Chem Lett, 2012, 3: 1885–1893
12 Ren Z, Wang J, Pan Z, *et al.* Amorphous TiO_2 buffer layer boosts efficiency of quantum dot sensitized solar cells to over 9%. Chem Mater, 2015, 27: 8398–8405
13 Ito S, Liska P, Comte P, *et al.* Control of dark current in photoelectrochemical (TiO_2/I^-–I^{3-}) and dye-sensitized solar cells. Chem Commun, 2005, 34: 4351–4353
14 Palomares E, Clifford JN, Haque SA, *et al.* Control of charge recombination dynamics in dye sensitized solar cells by the use of conformally deposited metal oxide blocking layers. J Am Chem Soc, 2003, 125: 475–482
15 Fei C, Tian J, Wang Y, *et al.* Improved charge generation and collection in dye-sensitized solar cells with modified photoanode surface. Nano Energy, 2014, 10: 353–362
16 Knez M, Kadri A, Wege C, *et al.* Atomic layer deposition on biological macromolecules: metal oxide coating of tobacco mosaic virus and ferritin. Nano Lett, 2006, 6: 1172–1177
17 Tallarida M, Das C, Schmeisser D. Quantum size effects in TiO_2 thin films grown by atomic layer deposition. Beilstein J Nanotechnol, 2014, 5: 77–82
18 Chandiran AK, Yella A, Stefik M, *et al.* Low-temperature crystalline titanium dioxide by atomic layer deposition for dye-sensitized solar cells. ACS Appl Mater Interface, 2013, 5: 3487–3493
19 Aarik J, Aidla A, Uustare T, *et al.* Morphology and structure of TiO_2 thin films grown by atomic layer deposition. J Crystal Growth, 1995, 148: 268–275
20 Knez M, Nielsch K, Niinistö L. Synthesis and surface engineering of complex nanostructures by atomic layer deposition. Adv Mater, 2007, 19: 3425–3438
21 Detavernier C, Dendooven J, Pulinthanathu Sree S, *et al.* Tailoring nanoporous materials by atomic layer deposition. Chem Soc Rev, 2011, 40: 5242–5253
22 Niu W, Li X, Karuturi SK, *et al.* Applications of atomic layer deposition in solar cells. Nanotechnology, 2015, 26: 064001
23 Kim JY, Lee KH, Shin J, *et al.* Highly ordered and vertically oriented TiO_2/Al_2O_3 nanotube electrodes for application in dye-sensitized solar cells. Nanotechnology, 2014, 25: 504003
24 Alibabaei L, Farnum BH, Kalanyan B, *et al.* Atomic layer deposition of TiO_2 on mesoporous nano ITO: conductive core–shell photoanodes for dye-sensitized solar cells. Nano Lett, 2014, 14: 3255–3261
25 Lee HBR, Mullings MN, Jiang X, *et al.* Nucleation-controlled growth of nanoparticles by atomic layer deposition. Chem Mater, 2012, 24: 4051–4059
26 Brennan TP, Ardalan P, Lee HBR, *et al.* Atomic layer deposition of CdS quantum dots for solid-state quantum dot sensitized solar cells. Adv Energy Mater, 2011, 1: 1169–1175
27 Tian J, Gao R, Zhang Q, *et al.* Enhanced performance of CdS/CdSe quantum dot cosensitized solar cells via homogeneous distribution of quantum dots in TiO_2 film. J Phys Chem C, 2012, 116: 18655–18662
28 Hamann TW, Martinson ABF, Elam JW, *et al.* Atomic layer deposition of TiO_2 on aerogel templates: new photoanodes for dye-sensitized solar cells. J Phys Chem C, 2008, 112: 10303–10307
29 Yu L, Li Z, Liu Y, *et al.* Synthesis of hierarchical TiO_2 flower-rod and application in CdSe/CdS co-sensitized solar cell. J Power Sources, 2014, 270: 42–52
30 Sommeling PM, O'regan BC, Haswell RR, *et al.* Influence of a $TiCl_4$post-treatment on nanocrystalline TiO_2 films in dye-sensitized solar cells. J Phys Chem B, 2006, 110: 19191–19197
31 Tian J, Zhang Q, Zhang L, *et al.* ZnO/TiO_2 nanocable structured photoelectrodes for CdS/CdSe quantum dot co-sensitized solar cells. Nanoscale, 2013, 5: 936–943
32 Gamelas JAF, Ferraz E, Rocha F. An insight into the surface properties of calcined kaolinitic clays: the grinding effect. Colloid Surf A-Physicochem Eng Asp, 2014, 455: 49–57
33 Mukhopadhyay P, Schreiber HP. Aspects of acid-base interactions and use of inverse gas chromatography. Colloid Surf A-Physicochem Eng Asp, 1995, 100: 47–71
34 Powar S, Wu Q, Weidelener M, *et al.* Improved photocurrents for p-type dye-sensitized solar cells using nano-structured nickel(ii) oxide microballs. Energy Environ Sci, 2012, 5: 8896–8900
35 Du J, Du Z, Hu JS, *et al.* Zn–Cu–In–Se quantum dot solar cells with a certified power conversion efficiency of 11.6%. J Am Chem Soc, 2016, 138: 4201–4209
36 Ren F, Li S, He C. Electrolyte for quantum dot-sensitized solar cells assessed with cyclic voltammetry. Sci China Mater, 2015, 58: 490–495
37 Ren Z, Wang Z, Wang R, *et al.* Effects of metal oxyhydroxide coatings on photoanode in quantum dot sensitized solar cells. Chem Mater, 2016, 28: 2323–2330
38 Hwang JY, Lee SA, Lee YH, *et al.* Improved photovoltaic response of nanocrystalline CdS-sensitized solar cells through interface control. ACS Appl Mater Interface, 2010, 2: 1343–1348
39 Kim B, Li Y, Jung H, *et al.* Enhanced interconnection of TiO_2 nanoparticles using atomic layer deposition for flexible dye-sensitized solar cells with plastic substrates. Nano Lett, 2014, 09: 1440011
40 Kern R, Sastrawan R, Ferber J, *et al.* Modeling and interpretation of electrical impedance spectra of dye solar cells operated under open-circuit conditions. Electrochim Acta, 2002, 47: 4213–4225
41 Nakade S, Kanzaki T, Wada Y, *et al.* Stepped light-induced transient measurements of photocurrent and voltage in dye-sensitized solar cells: application for highly viscous electrolyte systems. Langmuir, 2005, 21: 10803–10807

Acknowledgments This work was supported by the National Natural Science Foundation of China (51374029 and 5151101345), the Program for New Century Excellent Talents in the University (NCET-13-0668), and the Fundamental Research Funds for the Central Universities (FRF-TP-14-008C1).

Author contributions Shen T and Li B performed the materials synthesis, characterization and photoelectrochemical measurements. Shen T was involved analysis and discussion, and wrote the manuscript. Tian J and Cao G proposed the strategy, supervised the design of experiments and revised the manuscript.

Conflict of interest The authors declare that they have no conflict of interest.

Ting Shen is a PhD candidate in Advanced Material and Technology Institute, University of Science and Technology Beijing. Her research is focused on interfacial modification of multi-component quantum dot and its photovoltaic properties.

Jianjun Tian is a professor in Advanced Material and Technology Institute, University of Science and Technology Beijing. His current research is focused on quantum dot sensitized solar cells and perovskite solar cells.

Guozhong Cao is a Boeing Steiner Professor of Materials Science and Engineering, Professor of Chemical Engineering, and Adjunct Professor of Mechanical Engineering at the University of Washington. He has published more than 300 papers, 7 books and 4 proceedings. His recent research is mainly focused on solar cells, lithium-ion batteries, supercapacitors, and hydrogen storage.

超薄ALD层包覆TiO_2光阳极增加量子点太阳能电池的量子点吸附量和电荷收集效率

沈婷[1], 田建军[1*], 李波[1], 曹国忠[1,2*]

摘要 TiO_2纳米晶体具有稳定的化学性质和合适的能带结构, 因而被广泛应用在量子点太阳能电池的光阳极材料中. 但是, 其较多的表面缺陷和颗粒边界引起的严重复合限制了电池效率. 本文利用原子层沉积法(ALD)在TiO_2光阳极膜上沉积一层超薄TiO_2层. 实验结果表明, 这层超薄TiO_2层不仅减少了表面缺陷, 改善了颗粒间的连接性, 阻止了复合的发生, 提高了电子收集效率, 而且通过表面能的提升, 量子点的吸附量增加, 光捕获效率(LHE)也得以提高. 因此, 基于ALD修饰的TiO_2膜制备的太阳能电池的效率达5.07%, 明显优于没有ALD 修饰的电池(4.03%).